New aspects of the magnetic excitations in $HoCo_2$

A. Castets and D. Gignoux
Laboratoire Louis Néel, Centre Nationale de la Recherche Scientifique, 166 X 38042 Grenoble Cédex, France

B. Hennion
Laboratoire Léon Brillouin, B.P. No. 2, 91190 Gif-sur-Yvette, France

(Received 14 July 1981)

We have obtained new results about the magnetic excitation spectrum of $HoCo_2$ using inelastic neutron scattering. It has been possible to observe at 6 K a well-defined cobalt excitation mode up to 14 THz. The application of a magnetic field along the easy magnetization axis has revealed the longitudinal character of the excitation at 2 THz observed at 6 K. New modes below and above the rotation temperature have been measured. These results have been analyzed in a Green's-function formalism using the random-phase approximation to determine the crystalline electric field (CEF) and the exchange parameters. Despite the use of an extra quadrupolar term for the crystalline field it has not been possible to get a satisfactory agreement for the dispersion curves obtained, together with the macroscopic measurements. However, the values obtained $W=0.2983$ K and $x=-0.4839$ for the CEF parameters are in agreement with those determined by other authors. The exchange parameters have been determined as $J_{\text{Ho-Ho}}=0\pm0.0005$ THz, $J_{\text{Ho-Co}}=-0.07$ THz, and $J_{\text{Co-Co}}=9$ THz. The main discrepancy concerns $J_{\text{Ho-Co}}$ which may be determined from the gap of the cobalt mode or from the molecular field when the CEF transition levels are fitted regardless of the cobalt mode. The discrepancy suggests that it might be necessary to take into account a mixture of $3d$ and $4f$ magnetism at the very level of the exchange mechanism, including the itinerant character of the $3d$ electrons.

I. INTRODUCTION

In the past years several studies have been devoted to the determination by inelastic neutron scattering of the magnetic excitations in the cubic Laves phases RM_2 (R = rare-earth element, and M = transition metal).[1–4] These studies involved the general understanding of the $3d$ and $4f$ magnetism. $Ho_{0.88}Tb_{0.12}Fe_2$ and $ErFe_2$ were satisfactorily interpreted by means of a localized model for the iron atoms and a mean-field model for the rare-earth atoms. The Curie temperatures of these compounds are of the same order of magnitude as that of pure iron and this indicates the dominance of iron magnetism. Alternatively, in the RNi_2 compounds the nickel is not magnetic[5] and the effects due to the $3d$ electrons are expected to be weak.

The intermediate family of RCo_2 compounds exhibit particular magnetic properties which are connected to the onset of magnetism of the $3d$ cobalt electrons. YCo_2 and $LuCo_2$ are enhanced Pauli paramagnets, but if the alloy contains a rare-earth element which is magnetic, a cobalt magnetic moment is induced, which can reach $1\mu_B$ in $GdCo_2$.[6] Moreover, $DyCo_2$,[7] $HoCo_2$,[6] and $ErCo_2$ (Ref. 8) exhibit at the ordering temperature a first-order transition. All these properties observed in the RCo_2 compounds are associated with a collective $3d$ electron metamagnetism which is induced by the applied field and the molecular field due to the rare earth.

These compounds are good candidates to study the mixing of the effects due to the crystalline electric field ($4f$ electrons) and to the itinerant magnetism ($3d$ electrons). Such a cobalt behavior was predicted by Wolfarth and Rhodes[9]; it occurs when the Stoner criteria is almost fulfilled, and the Fermi level is in a region of strong positive curvature of the density of states. These characteristics of the band structure were confirmed by a calculation performed by Cyrot and Lavagna.[10]

In this paper we present the results of inelastic neutron scattering performed on a single crystal of $HoCo_2$. Below its Curie temperature (77 K), $HoCo_2$ orders ferrimagnetically with the cobalt moments antiparallel to the holmium ones. A change of the easy magnetization direction occurs around 14 K.[11,12] Below 11 K the magnetization is along the [110] direction, while above 16 K it becomes parallel to the [100] axis; between these temperatures the easy magnetization direction rotates continuously.

Initial results reported earlier[13] consisted of a determination of several transitions on both sides of the spin-reorientation temperature range and the observation of a broad scattering likely related to the cobalt magnetism. A tentative analysis failed because of the impossibility to account for both the inelastic

neutron results and the macroscopic experiments such as magnetization and torque measurements.

We have since obtained improved information on the magnetic excitations using a larger single crystal. In Sec. II the new experimental results at 6 K and 18 K are presented. In Sec. III we present the dynamical susceptibility theory used in our analysis and in Sec. IV we discuss and compare the theoretical and experimental results.

II. EXPERIMENTAL

$HoCo_2$ crystallizes in the cubic $MgCu_2$-type Laves phase structure (space group $Fd3m$) with a lattice parameter of 7.17 Å. A single crystal of $HoCo_2$ was grown using a Chokralsky method and annealed for two days. The resulting ingot was then cut in order to obtain slabs 1.5 mm thick with a [110] axis perpendicular to the surface. Four slabs were mounted together to obtain a $1.5 \times 30\text{-mm}^3$ sample with a $[1\bar{1}0]$ vertical axis.

Neutron inelastic scattering measurements were performed in the Laue-Langevin Institute, using the triple axis spectrometers IN1 and IN8 situated on a hot and thermal source, respectively. The magnetic excitations have been studied in the [001] and [111] directions. Since the results observed in the two directions were very similar, we decided, in order to minimize the effects of the sample absorption, to study the [001] direction. The temperature dependence of the magnetic excitations has been investigated both around the spin-reorientation temperature (14 K) and the Curie temperature (77 K).

The dispersion curves obtained at 6 and 18 K which have already been published[13] have been confirmed and extended. The overall results are reported on Figs. 1 and 2. The new features to be outlined are the following:

(1) In order to improve the interpretation of the results we have attempted to identify the longitudinal or transverse character of some of the magnetic exci-

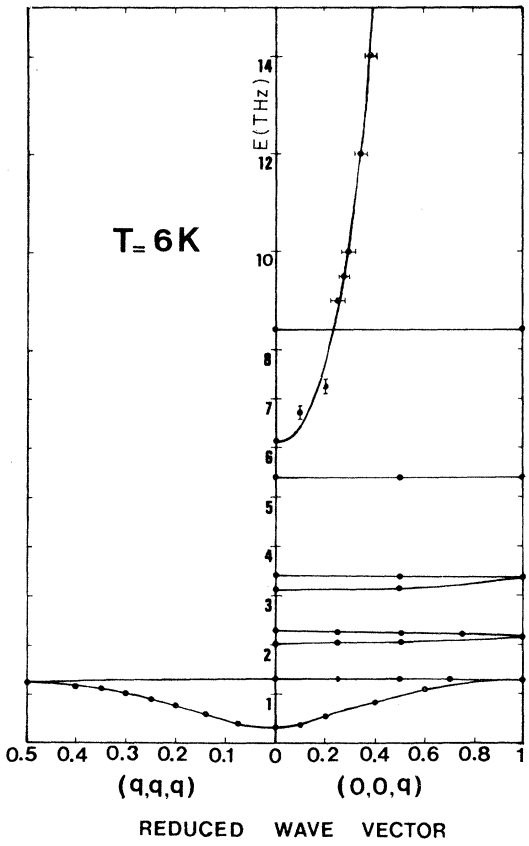

FIG. 1 Magnetic excitations in $HoCo_2$ observed at 6 K along the [111] and [001] directions. Full lines are eye-guide lines. The line following the cobalt experimental points is drawn using an analytic law $\omega = \omega_0 + Dq^2$ with $\omega_0 = 6.1$ THz and $D = 62$ THz Å^2.

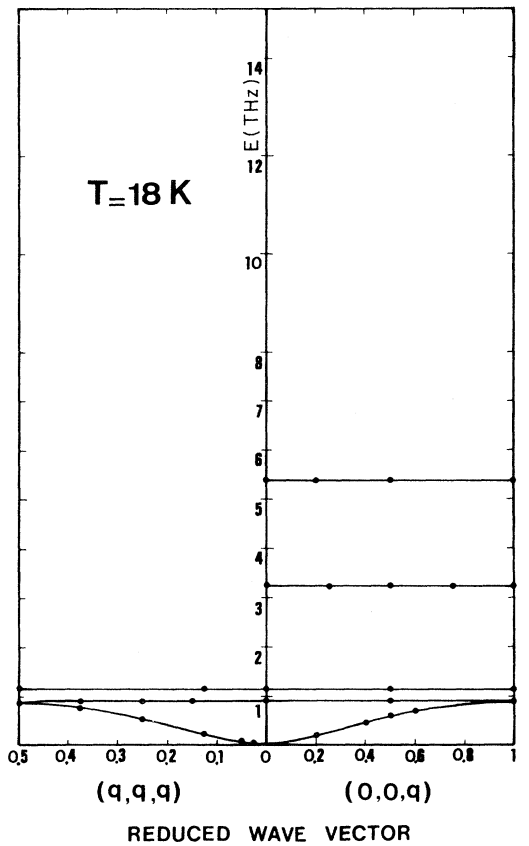

FIG. 2. Magnetic excitations in $HoCo_2$ observed at 18 K along the [111] and [001] directions. Full lines are eye-guide lines.

tations. This was carried out by making measurements in which a magnetic field was applied along the easy magnetization axis and perpendicular to the scattering vector. Owing to the orientation factor $1+(-)K_z^2$ in the cross section, K_z being the projection of the magnetization direction along the scattering direction, the intensity of a longitudinal mode must increase from $\frac{2}{3}$ (polydomain sample without field) to 1 (monodomain sample with field); similarly, under the same conditions the intensity of a transverse mode must decrease from $\frac{4}{3}$ to 1.

The sample was mounted in a permanent magnet as shown on Fig. 3. The magnetic field provided by permanent magnets of $SmCo_5$ was about 3.5 kOe on the sample. The experiment without field was achieved by removing the $SmCo_5$ magnets. Due to the low field and to the particular shape of the sample, the theoretical intensity ratio could not be obtained. However, the behavior of the intensity (increasing or decreasing), which is illustrated in Fig. 4, allowed us to ascertain the character of the observed modes. This method has essentially been used to determine the polarization of the 2.1-THz mode observed at 6 K, which appears to be longitudinal. Unfortunately, this requires the use of only half the sample and the resulting lack of time prevented us from complete analysis of the upper transitions.

(2) At 6 K, the mode at 5 THz, which was tentatively proposed in the previous publication, has been confirmed, and a new mode at 8.4 THz has been revealed. At 18 K a new mode at 5.4 THz has also been measured. But we could not determine the character of any of these modes.

(3) The broad scattering previously observed around the 004 Brillouin zone has been resolved; a dispersive excitation has been found which starts from 6.1 ± 0.3 THz at $q=0$ and which could be followed up to 14 THz (see Fig. 1). On Fig. 5 is shown one of the neutron groups obtained by constant energy scans in the 004 Brillouin zone. The full line indi-

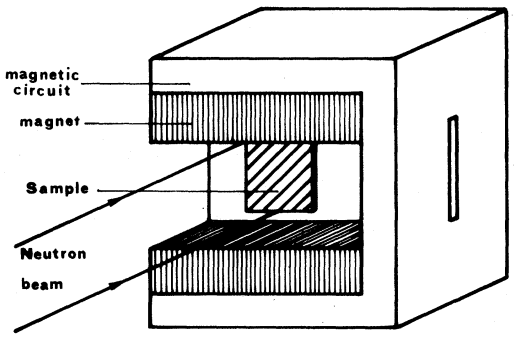

FIG. 3. Sample holder used to apply a magnetic field along the easy magnetization axis. The magnetic field is provided by permanent magnets of $SmCo_5$.

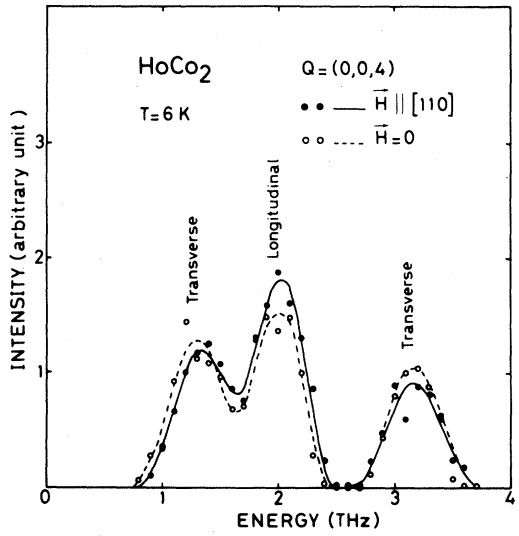

FIG. 4. Constant q scan observed at 6 K at $Q=(0,0,4)$. ——: magnetic field along the [110] vertical axis. – – –: without magnetic field. The lines are the results of a least-squares fit taking into account the resolution function of the spectrometer. The mode at 1.2 THz should not be observed in the 004 Brillouin zone. In the conditions of the observation its intensity seems to be field independent. For the modes at 2 and 3.17 THz the intensity ratios correspond to about 60% domain alignment. In the figure the background is subtracted from the intensity.

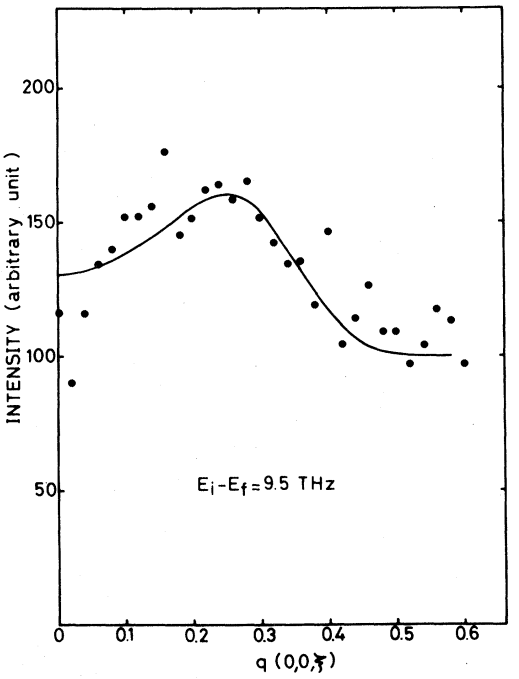

FIG. 5. Constant energy scan at 9.5 THz. The full line is calculated in accordance with a dispersion law $\omega=\omega_0+Dq^2$ ($\omega_0=6.1$ THz and $D=62$ THz Å^2) after taking into account the experimental resolution.

cates the intensity calculated for a dispersion law of the form $\omega = \omega_0 + Dq^2$, with $\omega_0 = 6.1 \pm 0.2$ THz and $D = 62 \pm 3$ THz Å^2, when taking into account the experimental resolution. Scans above the Curie temperature indicate that this dispersive mode disappears in the paramagnetic phase.

The dispersion of this mode within this energy range and its temperature variation clearly demonstrate that it must be attributed to the magnetism of the cobalt atoms. The gap observed at $q = 0$ corresponds to the action of the molecular field due to holmium ions on cobalt ions.

A numerical analysis of these data, taking into account the resolution function of the spectrometer, allowed us to determine an intrinsic linewidth of about 0.3 THz for the $q = 0$ mode at 6.1 THz. However, as the scans at higher energies have been performed at constant energy and in rather bad focusing conditions because of experimental constraints, we could not analyze the evolution of this linewidth with energy.

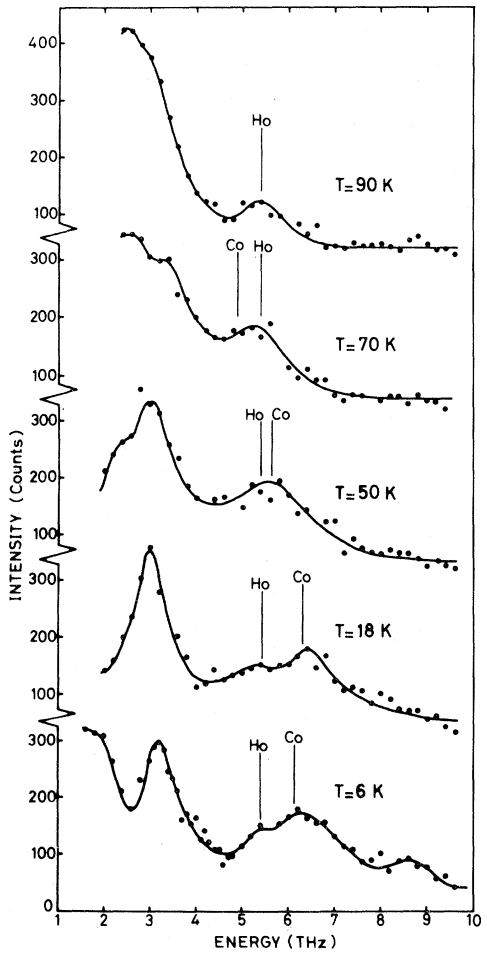

FIG. 6. Thermal variation of the excitations measured at $q = 0$.

Finally, we have performed some measurements with a variation of temperature up to 90 K. The excitations at $q = 0$ have been measured at 50, 72, and 90 K, and the results are compared to those at 6 and 18 K in Fig. 6. The main features which can be outlined are as follows:

(1) The appearance at about 2.5 THz of a new mode which corresponds to the increase with temperature of the population of an excited state.

(2) The cobalt mode moves towards lower energies when the temperature increases (this corresponding to the renormalization of J_z^{Ho} with temperature). This mode disappears at 90 K. However, the behavior of these transitions is peculiar because the observations below and above the Curie temperature (77 K) are not very different.

III. DYNAMICAL SUSCEPTIBILITY THEORY

In order to analyze the experimental results we used the dynamical susceptibility theory for a many-level system developed by Buyers, Holden and Perreault (1975).[14] We have extended this theory to take into account the fact that there are six atoms per unit cell and that the cobalt and holmium moments are antiparallel. We have therefore used the following Hamiltonian

$$H = \sum_i H_{\mathrm{CEF}}(i) - 2\sum_{i,j} J_{ij}\vec{S}_i \cdot \vec{s}_j - 2\sum_{i>i'} J_{ii'}\vec{S}_i \cdot \vec{S}_{i'} - 2\sum_{j>j'} J_{jj'}\vec{s}_j \cdot \vec{s}_{j'} , \quad (1)$$

which contains a crystalline-electric-field term for the holmium ions and exchange terms between holmium-holmium, holmium-cobalt, and cobalt-cobalt ions. For the sake of simplicity, all the exchange terms are of the Heisenberg type. The indices i and j refer, respectively, to holmium and cobalt ions and the position $\vec{r}$ of an ion will be given by $\vec{r} = \vec{l} + \vec{\nu}$, where $\vec{l}$ defines the origin of the cell and $\vec{\nu}$ the position within the cell. To specify whether the ion is an holmium or a cobalt one, we use $\vec{\imath}$ and $\vec{\lambda}$ for the holmium and $\vec{\jmath}$ and $\vec{\mu}$ for the cobalt. The total angular momentum of any ion will be written $\vec{J}$ and when we want to specify an holmium or cobalt ion we will use $\vec{S}$ or $\vec{s}$.

It is known (see Marshall and Lovesey[15]) that the inelastic neutron scattering cross section is proportional to the imaginary part of the generalized dynamical susceptibility

$$I = \sum_{\alpha,\beta} (\delta_{\alpha\beta} - K_\alpha K_\beta) \frac{e^{\hbar\omega/k_B T}}{e^{\hbar\omega/k_B T} - 1} \times \mathrm{Im}[G^{\alpha\beta}(\vec{Q}, \omega)] , \quad \alpha, \beta = x, y, z . \quad (2)$$

As we are dealing with a cubic crystal with collinear momentum, this intensity can be separated into long-

itudinal and transverse parts with

$$I^{\text{long}}\alpha(1-K_z^2)\frac{e^{\hbar\omega/k_BT}}{e^{\hbar\omega/k_BT}-1}\,\text{Im}G^{zz}(\vec{Q},\omega) \quad , \tag{3}$$

$$I^{\text{trans}}\alpha(1+K_z^2)\frac{e^{\hbar\omega/k_BT}}{e^{\hbar\omega/k_BT}-1} \times \text{Im}[G^{+-}(\vec{Q},\omega)+G^{-+}(-\vec{Q},\omega)] \quad . \tag{4}$$

Let us first focus our attention on the transverse Green's functions. In the present case in which we have several ions, the Green's function $G^{\alpha\beta}(\vec{Q},\omega)$ may be defined in terms of partial Green's functions as

$$G^{\alpha\beta}(\vec{Q},\omega)=\sum_{\nu\nu'}\exp -i\vec{\tau}(\vec{\nu}-\vec{\nu}')\,G_{\nu\nu'}^{\alpha'\beta'}(\vec{q},\omega) \quad , \tag{5}$$

where $\vec{\tau}$ is a reciprocal-lattice vector such that $\vec{Q}=\vec{\tau}+\vec{q}$. Because of the antiparallelism of holmium and cobalt, $\alpha'(\beta')$ will be $\alpha(\beta)$ when $\nu(\nu')$ designates an holmium ion and $-\alpha(-\beta)$ when $\nu(\nu')$ designates a cobalt ion. The general expression of $G_{\nu\nu'}^{\alpha\beta}(\vec{q},\omega)$ is

$$G_{\nu\nu'}^{\alpha\beta}(\vec{q},\omega)=\frac{1}{N}\sum_{ll'}\exp -i\vec{q}(\vec{r}-\vec{r}') \times G_{\nu\nu'}^{\alpha\beta}(ll',\omega) \tag{6}$$

and the $G_{\nu\nu'}^{\alpha\beta}(ll',\omega)$ is the time-dependent Fourier transform of $G_{\nu\nu'}^{\alpha\beta}(ll',t)$ defined by

$$G_{\nu\nu'}^{\alpha\beta}(ll',t)=-i\Theta(t)\langle[J_\nu^\alpha(l,t),J_{\nu'}^\beta(l',0)]\rangle \quad . \tag{7}$$

The problem is now to obtain the $G_{\nu\nu'}^{\alpha\beta}(\vec{q},\omega)$ in the case of the above Hamiltonian. For this we will use the Heisenberg equation of motion, the general form of which is

$$\omega G(A,B,\omega)=\langle[A,B]\rangle+G([A,H],B,\omega) \quad . \tag{8}$$

Thus we must solve a set of equations by using some approximations to decouple higher-order Green's functions, which appear in the equation of motion. For this we follow the procedure used by Buyers *et al.*[14]

The first step is to separate the Hamiltonian into a single-ion part, including crystalline electric field terms and the exchange terms in the molecular-field approximation, and an interionic part consisting of exchange terms corrected of the molecular field. The single-ion part, which concerns only the Ho, is diagonalized and written

$$H_1=\sum_{i,\lambda}\sum_n\omega_n C_n^\dagger(i,\lambda)C_n(i,\lambda) \quad , \tag{9}$$

where the operator $C_n(i)$ annihilates the state $|n\rangle$ of energy ω_n at site $\vec{i}+\vec{\lambda}$. The remaining interionic part is

$$H_2=-2\sum_i S_i^\zeta\left(\sum_{i'}J_{ii'}(S_{i'}^\zeta-\langle S_{i'}^\zeta\rangle)-\sum_j J_{ij}(s_j^\zeta-\langle s_j^\zeta\rangle)\right)-\sum_{ii'}J_{ii'}(S_i^+S_{i'}^-+S_i^-S_{i'}^+) -\sum_{ij}J_{ij}(S_i^+s_j^++S_i^-s_j^-)-\sum_{ij}J_{ij}(s_j^+S_i^++s_j^-S_i^-)-\sum_{jj'}J_{jj'}(s_j^+s_{j'}^-+s_j^-s_{j'}^++2s_j^\zeta s_{j'}^\zeta) \quad . \tag{10}$$

According to the type of ion in the left part of the Green's function we will distinguish two types of expansion:

(1) $G_{\lambda\nu}^{\alpha\beta}(\vec{q},\omega)$. The spin operators of the holmium ions may be developed on the basis of $C_n^\dagger C_n$ giving

$$S^\alpha(r)=\sum_{mn}S_{mn}^\alpha(\lambda)C_m^\dagger(i,\lambda)C_n(i,\lambda) \quad . \tag{11}$$

Then $G_{\lambda\nu}^{\alpha\beta}(il,t)$ may be developed in

$$G_{\lambda\nu}^{\alpha\beta}(il,t)=\sum_{mn}S_{mn}^\alpha(\lambda)\hat{G}_{\lambda\nu,mn}^\beta(il,t) \tag{12}$$

with

$$\hat{G}_{\lambda\nu}^\beta(il,t)=-i\Theta(t)\langle[C_m^\dagger(i,\lambda)C_n(i,\lambda),J_\nu^\beta(1,0)]\rangle \quad , \tag{13}$$

Following Buyers we use the commutation rules between the C's and the random-phase approximation to decouple the terms including four operators. For the time and spatial Fourier transform $G_{\lambda\nu}^{\alpha\beta}(\vec{q},\omega)$ this yields after some algebra

$$G_{\lambda\nu}^{\alpha\beta}(\vec{q},\omega)=g_\lambda^{\alpha\beta}(\omega)\delta_{\lambda\nu}-g_\lambda^{\alpha+}(\omega)\left(\sum_{\lambda'}J_{\lambda'\lambda}(\vec{q})G_{\lambda'\nu}^{-\beta}(\vec{q},\omega)+\sum_\mu J_{\mu\lambda}(\vec{q})G_{\mu\nu}^{+\beta}(\vec{q},\omega)\right) -g_\lambda^{\alpha-}(\omega)\left(\sum_{\lambda'}J_{\lambda'\lambda}(\vec{q})G_{\lambda'\nu}^{+\beta}(\vec{q},\omega)+\sum_\mu J_{\mu\lambda}(\vec{q})G_{\mu\nu}^{-\beta}(\vec{q},\omega)\right) \quad , \tag{14}$$

where

$$g_\lambda^{\alpha\beta}(\omega)=\sum_{mn}\frac{S_{mn}^{\alpha}(\lambda)S_{nm}^{\beta}(\lambda)(f_m-f_n)}{\omega-\omega_n+\omega_m} \tag{15}$$

is the single-site dynamical susceptibility;

$$f_n=\exp(-\omega_n/k_BT)\Big/\left(\sum_m\exp(-\omega_m/k_BT)\right) \tag{16}$$

and

$$J_{\nu\nu'}(\vec{q})=\sum_{(\nu'-\nu)}J_{\nu\nu'}\exp[i\vec{q}(\vec{\nu}'-\vec{\nu})] \ . \tag{17}$$

(2) For the Green's functions such as $G_{\mu\nu}^{\alpha\beta}(\vec{q},\omega)$ we use the commutation relations between the s operators and the usual random-phase approximation to decouple terms as $s^{\zeta}s^{+}$. And we get

$$G_{\mu\nu}^{\alpha\beta}(\vec{q},\omega)=g_\mu^{\alpha\beta}(\omega)\delta_{\mu\nu}\delta_{\alpha-\beta}-g_\mu^{\alpha\beta}(\omega)\sum_\lambda J_{\lambda\mu}(\vec{q})G_{\lambda\nu}^{(-\alpha)\beta}(\vec{q},\omega)-g_\mu^{\alpha\beta}(\omega)\sum_{\mu'}J_{\mu'\mu}(\vec{q})g_{\mu'\nu}^{\alpha\beta}(\vec{q},\omega) \tag{18}$$

with

$$g_\mu^{\alpha\beta}(\omega)=\frac{2\alpha\langle s_\mu^{\zeta}\rangle}{\omega+2\alpha\left(\sum_\lambda J_{\lambda\mu}\langle S_\lambda^{\zeta}\rangle-\sum_{\mu'}J_{\mu\mu'}\langle s_\mu^{\zeta}\rangle\right)} \ . \tag{19}$$

Gathering all the results we can write the system of linear equations as

$$\overline{M}(\omega)\vec{G}=\vec{g} \ . \tag{20}$$

So the solution of our problem will be given by

$$\vec{G}=\overline{M}^{-1}(\omega)\vec{g} \ . \tag{21}$$

As the magnetic excitations we are looking for are defined by the poles of the generalized dynamical susceptibility, we see on the last equation that we will get these poles by looking for values ω such that

$$\det[\overline{M}(\omega)]=0 \ . \tag{22}$$

Because of the symmetry of the problem, the matrix $\overline{M}$, which is of rank 72, will be reduced, and, in fact, we have to work with a 12×12 matrix.

In order to calculate the intensity of the neutron groups, it is first necessary to obtain a pole ω and then to add a small imaginary part $i\epsilon$ to ω and compute

$$\lim_{\epsilon\to0}\mathrm{Im}[\epsilon\overline{M}^{-1}(\omega+i\epsilon)\vec{g}(\omega+i\epsilon)] \ .$$

If the value of ϵ is small enough the result is independent of ϵ. In the present case the computations were performed using $\epsilon=0.001$ K.

Let us consider briefly the longitudinal part of the intensity. The calculation of the longitudinal Green's function, provided we are only concerned with holmium atoms, yields

$$G_{\lambda\lambda'}^{zz}(q,\omega)=g_\lambda^{zz}(\omega)\delta_{\lambda\lambda'}+2g_\lambda^{zz}(\omega)\times\sum_{\lambda''}J_{\lambda''\lambda}(\vec{q})G_{\lambda''\lambda'}^{zz} \ . \tag{23}$$

In the unit cell there are two holmium atoms which are identified as 1 and 2. The spin waves are then the solutions of the equation

$$1-4[g_{\mathrm{Ho}}^{zz}(\omega)]^2|J_{\mathrm{Ho}_1-\mathrm{Ho}_2}(\vec{q})|^2=0 \ . \tag{24}$$

The calculation of the intensity is then straightforward using the previous equation.

IV. ANALYSIS OF THE EXPERIMENTAL RESULTS

The previous model requires a knowledge of several parameters. First, a knowledge of the exchange integrals, is required which may be limited to the first nearest neighbors: J_1 for Ho-Ho exchange, J_2 for Ho-Co, and J_3 for Co-Co. Second, the parameters involved in the crystal-field Hamiltonian are required. In the cubic symmetry this Hamiltonian is written[16]

$$H_c=\frac{Wx}{F_4}(O_4^0+5O_4^4)+\frac{W}{F_6}(1-|x|)(O_6^0-21O_6^4) \ , \tag{25}$$

where the O_l^m are the Stevens operators, F_4 and F_6 are coefficients depending only on the rare-earth ion, and W, x are adjustable parameters.

Thus we have to determine these parameters using the following experimental results: magnetization and torque measurements, temperature of spin rotation, and neutron inelastic scattering measurements at different temperatures. The latter experiments give direct information about the transitions between crystal-field levels and the dispersion of these levels. Calculation of dispersion curves were undertaken using, as far as possible, a constraint imposed by the temperature at which spin rotation takes place. A further constraint used in the calculation was the zone boundary energies of first three modes observed at 6 and 18 K. It should be recalled that at 6 K the second mode has a longitudinal character, and at 18 K the second mode corresponds to a transition between first and second excited-crystal-field levels.

From our neutron inelastic scattering measure-

ments, J_1 can be determined directly. Since there are two holmium ions per unit cell, the magnetic excitation observed at the zone boundary is degenerate and can be separated into "in-phase" and "out-of-phase"[22] modes. These excitations are observed in different Brillouin zones depending on whether the magnetic elastic structure factor is maximum or minimum, respectively. The calculations then, show that the dispersion of the "out-of-phase" mode depends only on J_1. As these modes are almost flat, we deduce that the value of J_1 is small and certainly less than 10^{-3} THz.

Using the model described above, we have refined the crystal-field and exchange (J_2 and J_3) parameters, in order to fit the whole experimental data. The best agreement has been obtained with the crystal-field paratmeters previously given by Gignoux *et al.*[11] (Table I) and with $J_2=-5.1\times10^{-2}$ THz and $J_3=0.6$ THz. The value of J_2 obtained is consistent with the value of the molecular field acting on holmium ions reported by Gignoux. The calculated dispersion curves at 6 and 18 K are compared with the experimental points in Figs. 7 and 8, respectively. The agreement is particularly good for the acoustic mode. This is rather satisfactory since magnetization and torque measurements as well as the acoustic mode are characterized by the low-lying energy levels of the holmium ion. The other flat modes at higher energies are also in excellent agreement with our model calculation, but the dispersion curve for the cobalt ions does not correspond to the observed curve. In particular, the calculated gap (3.5 THz at 6 K) and the stiffness constant (5 THz Å^2 at 6 K) are much smaller than the experimental values (6.1 THz and 62 THz Å^2). Prompted by this discrepancy, we decided to reformulate the problem by first considering the mode associated with the cobalt. In the localized model used the cobalt mode depends only on J_2 and J_3. It is then possible to determine these exchange integrals from the neutron experimental results: the gap at $q=0$ of the cobalt mode depends essentially on J_2. A calculation within the spin wave approximation, even when the itinerant character of the cobalt magnetism is taken into account,[17] shows that the gap of the optic mode can be written

$$-12J_2(\langle S_z\rangle-2\langle s_z\rangle)\ . \tag{26}$$

This gives a value for J_2 of -7.4×10^{-2} THz.

Then we can determine the molecular field acting on the holmium ions using the expression

$$H_{ex}=(-24J_2\langle s_z\rangle+8\langle S_z\rangle J_1)/g_J\ , \tag{27}$$

which yielded $H_{ex}=500$ kOe if J_1 is assumed to be zero, $\langle s_z\rangle=0.5$, and $\langle S_z\rangle=7.5$. The stiffness constant D of the cobalt mode is related to J_3 and a comparison with the experimental curve yields $J_3=9.8$ THz. With these exchange integrals the cobalt mode is well accounted for, but it has not been possible to obtain a set of crystal-field parameters which also give a satisfactory fit of the lower-energy modes.

Thus the model including crystal-field and exchange effects is not able to give a satisfactory picture of the whole experimental data.

In order to improve the model, the next possible step is to introduce terms of higher order than the Heisenberg exchange term. Indeed the existence of quadrupolar terms has already been suggested in other rare-earth transition-metal compounds such as $TbCo_2$ (Ref. 18) and in rare-earth cubic compounds of the CsCl type,[19] in relation to the distortion observed in these materials. This quadrupolar contribution can include two terms: a quadrupolar exchange term and a magnetoelastic term: H_Q+H_{me}. If we write the quadrupolar exchange Hamiltonian H_Q in the mean-field approximation, it becomes isomorphous and indistinguishable from the magnetoelastic

TABLE I. Comparison of the results obtained in different RCo_2 compounds.

Compound	$J_{T\text{-}T}$ (THz)	$J_{R\text{-}T}$ (THz)	A_4^0 (THz/a_0^4)	A_6^0 (THz/a_0^6)	Reference
$HoCo_2$	0.6	-5.1×10^{-2}	2.40	−0.082	11 and this study without quadrupolar term
$HoCo_2$	9.8	-7.0×10^{-2}	1.26	−0.039	This study with quadrupolar terms
$HoCo_2$		-5.3×10^{-2}	1.04	−0.048	21
$ErCo_2$		-3.7×10^{-2}	1.04	−0.034	22
$TbCo_2$		-8.7×10^{-2}	1.11	−0.063	18
$TmCo_2$		-1.9×10^{-2}	3.22	−0.063	23

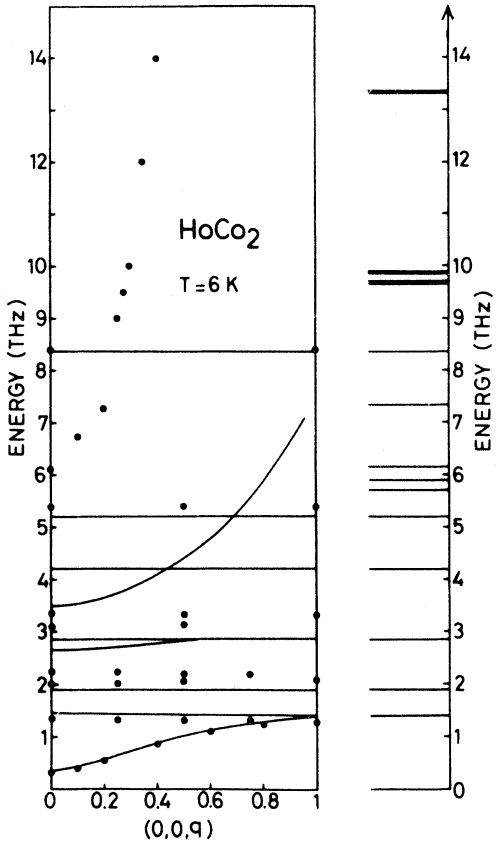

FIG. 7. Magnetic excitations in $HoCo_2$ at 6 K compared to the model calculation, with $W=0.6$ K, $x=-0.4665$, $H_{ex}=334$ kOe, $J_{Ho\text{-}Ho}=0.5\times10^{-3}$ THz, $J_{Ho\text{-}Co}=-5.1\times10^{-2}$ THz, and $J_{Co\text{-}Co}=0.6$ THz. For sake of simplicity we have only represented the curves calculated in the $[00q]$ direction. The splitting of $^5J_8$ multiplet of the Ho^{3+} at this temperature is shown on the right of the corresponding dispersion curve.

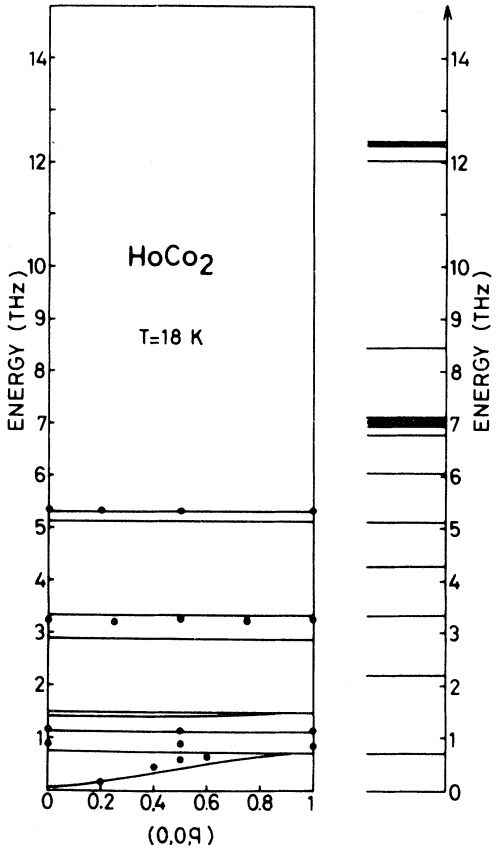

FIG. 8. Magnetic excitations in $HoCo_2$ at 18 K compared with the curves calculated in the same conditions as Fig. 7.

Hamiltonian H_{me}.[20] Then we have

$$H_Q+H_{me}$$
$$=-\sum_{i\neq i'}G_1(i,i')[O_2^0(i)O_2^0(i')+3O_2^2(i)O_2^2(i')]$$
$$-\sum_{i\neq i'}G_2(i,i')[P_{xy}(i)P_{xy}(i')+P_{yz}(i)P_{yz}(i')+P_{zx}(i)P_{zx}(i')]\ , \tag{28}$$

where O_2^0, O_2^2, and P_{ij} are the second-order Steven's operators

$$O_2^0=2J_z^2-J(J+1)\ ,\quad O_2^2=J_x^2-J_y^2\ ,$$
$$P_{ij}=\tfrac{1}{2}(J_iJ_j+J_jJ_i)\ ,\quad i,j=xy,\ yz,\ \text{and}\ zx\ .$$

With this additional exchange term it has been possible to find several sets of parameters W, x, G_1, and G_2 which reasonably, but not perfectly, account for the observed excitations, the temperature range of the spin rotation, and the gap of the cobalt mode. The observed excitations above 3 THz are more or less accounted for depending on the assumption made for their character, longitudinal or transverse. However there still remains a systematic discrepancy as regards the temperature dependence of the magnetization anisotropy.

We did not consider the relative intensities of the modes as an essential criterion because of several experimental anomalies. For instance, the first excited level which is an "out-of-phase" mode has been observed around the 004 Brillouin zone, which is, according to the magnetic structure factor, a "forbidden" zone. Furthermore, in any calculation, contrary to the experiment, the first longitudinal excitation has a low intensity.

In all the sets of parameters that we obtained, G_1 and G_2 are negative. Furthermore, G_2 is one order of magnitude greater than G_1. If the origin of G_1

and G_2 was purely magnetoelastic their value would be positive.[20] This shows the preponderance of the negative quadrupolar exchange. We have then assumed that all the contribution to the quadrupolar term was of exchange origin. At this step we have to estimate the influence on the dispersion of the modes of this additional exchange contribution. This can be done within the framework of the Green's function formalism, and the subsequent calculations are presented in the Appendix.

The main result of this calculation is that the quadrupolar exchange term introduces a noticeable dispersion on the "out-of-phase" mode. This is exemplified in Figs. 9 and 10 where the results of the calculation performed are presented with $W=0.3$ K, $x=-0.48$, $H_{ex}=500$ kOe, $G_1=-2.7$ mK, and $G_2=-11.7$ mK which is one of the solutions with the smallest G_1 and G_2. Even in this case the dispersion introduced by the quadrupolar terms should have been observed experimentally.

The dispersion could be compensated by enhancing the Heisenberg exchange J_1 between holmium ions. But on the one hand, if we consider the molecular field as a constant, this would imply a decrease of J_2 and consequently a lowering of the gap of the cobalt mode; and on the other hand it would seem quite artificial to introduce two independent exchange terms the effects of which would compensate each other. Nevertheless it might happen that a unique phenomenon gives rise simultaneously to two kinds of exchange with such a compensation. So the exact determination, of the CEF remains unsettled.

In Table I we compare our results with those obtained in different RCo_2 compounds. For the crystal-field parameters we have reported the values of A_4^0 and A_6^0 because they should be at first order independent of the rare earth. The A_4^0 reported in this table are in the same range, except for $TmCo_2$. However, for the A_6^0 values this is not obviously observed. Concerning $HoCo_2$, it is interesting to point out that although the values of A_4^0 and A_6^0 determined after introducing the quadrupolar terms are a factor of 2 smaller than those determined without these terms, the ratio A_4^0/A_6^0 is nearly the same. In fact, the rotation temperature which has been taken into account is very sensitive to this ratio. The A_4^0 and A_6^0 parameters determined by Koon and Rhyne[21] are a little different from ours but they give a rota-

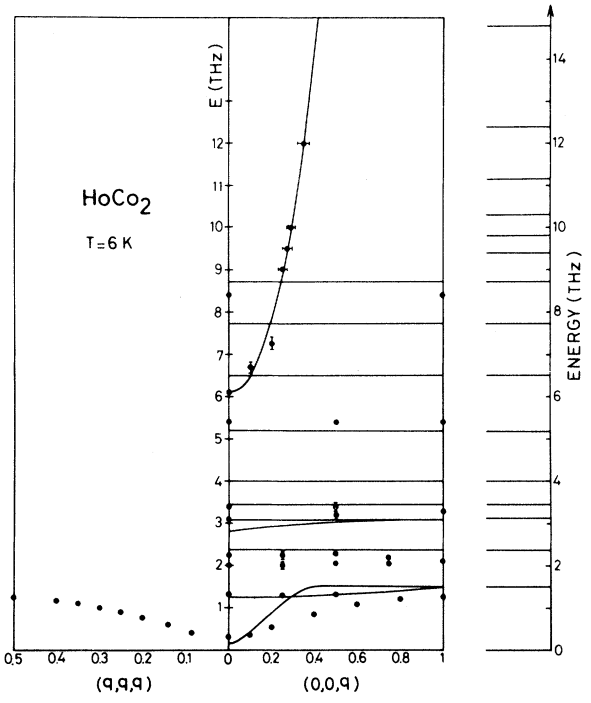

FIG. 9. Magnetic excitations in $HoCo_2$ at 6 K compared to the model calculation using the following parameters: $W=0.3$ K, $x=-0.48$, $H_{ex}=500$ kOe, $G_1=-2.7\times10^{-3}$ K, $G_2=-11.7\times10^{-3}$ K, $J_{Ho\text{-}Ho}=0.5\times10^{-3}$ THz, $J_{Ho\text{-}Co}=-7\times10^{-2}$ THz, and $J_{Co\text{-}Co}=9.8$ THz.

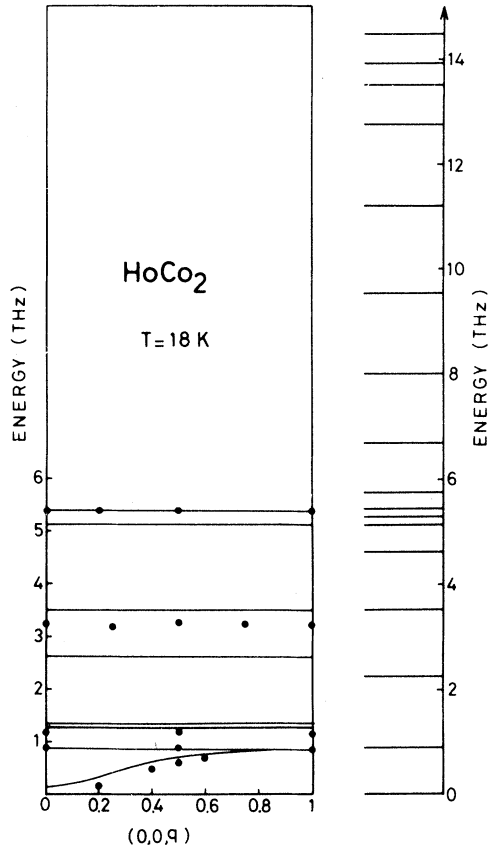

FIG. 10. Magnetic excitations in $HoCo_2$ at 18 K compared with the curve calculated in the same conditions as Fig. 9.

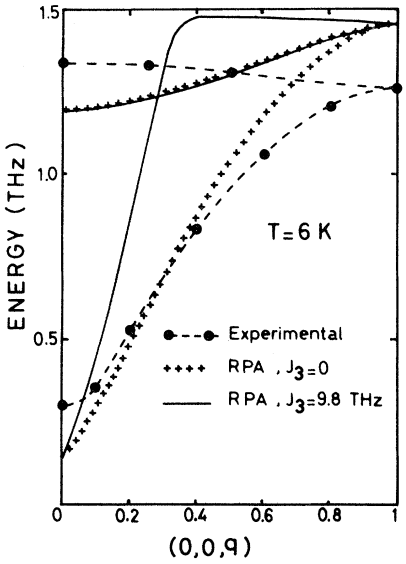

FIG. 11. Fit at 6 K of the lowest transition in the same conditions as Fig. 9, except the value of $J_{Co\text{-}Co}$ which is 9.8 THz in the case of the solid line and 0 THz for the dotted line. (– – – is an eye-guide line through the experimental points.)

tion temperature much higher because the ratio A_4^0/A_6^0 is different.

Another aspect of the problem concerns the cobalt-cobalt interaction J_3. In the localized picture presented previously, this interaction not only gives rise to the parabolic cobalt mode, but it also influences the dispersion of the acoustic mode. In fact the value of 9.8 THz for J_3, provided by the cobalt mode, gives rise in the acoustic mode to a dispersion stronger than that observed. This is illustrated in Fig. 11 where the experimental acoustic curve corresponds to a nearly zero value of J_3. This is undoubtedly related to the itinerant character of the cobalt magnetism. The spin-wave stiffness constant is directly related to the band structure via the electronic density of states and the relevant parameter is the splitting between up an down sub-bands which corresponds to an intra-atomic exchange between d electrons on the same site. Consequently, in that context the concept of J_3 is not really meaningful.

V. CONCLUSION

The measurements on $HoCo_2$ have provided a lot of results. They may qualitatively be related either to CEF effects, such as the spin reorientation temperature and the flat modes observed in the inelastic neutron scattering experiments, or to itinerant magnetism effects, such as the first-order character of the ferro-para transition and the parabolic spin-wave dispersion curve. They also have revealed some anomalies: observation of modes in forbidden zones, high intensity of a longitudinal mode, and temperature dependence of the transition levels around the Curie temperature.

Even though it is possible to get a partial agreement by considering only some of the observations, we did not succeed in getting a satisfactory agreement of the all of the results.

As far as the cobalt is concerned, the situation seems to be relatively simple; it corresponds to that of an itinerant ferromagnet in the molecular field of holmium ions. It can be accounted for with two parameters: a stiffness constant $D = 62$ THz Å^2 which reflects band-structure properties and an antiferromagnetic exchange between holmium and cobalt of about 7×10^{-2} THz. This determination of the holmium-cobalt exchange interaction is in principle quite direct and depends only on the average magnetic moment of holmium and cobalt, which is known by other measurements. However, it is responsible for the main discrepancy revealed by the analysis of the CEF results. Indeed if we consider only the CEF results, regardless of the cobalt mode, and try to adjust, W, x, and H_{ex} (as did Gignoux *et al.*[11] or Koon and Rhyne[22]), we obtain a fair agreement, with a H_{ex} value which is about 1.5 times smaller than that determined using the quadrupole terms.

Such a situation was not encountered in the other compounds already studied, because, in the RFe_2, only one flat mode has been observed in addition to the iron spin wave and in the RCo_2 systems no cobalt mode has been observed. Thus a cross determination of the rare-earth-metal exchange could not be performed. However in the case of $ErCo_2$, Koon and Rhyne[22] state that they have looked for the cobalt mode in an energy range extrapolated from their determination of J_2 via H_{ex}. It would be quite interesting to look at higher energies to see if indeed the cobalt mode does occur, thus revealing the same discrepancy as in $HoCo_2$.

Finally, if we add the anomalies already outlined and the weakness of the interactions between holmium ions, which is not consistent with the value of the Curie temperature of $HoNi_2$ where the nickel is not magnetic, all these facts suggest that it might be necessary to have a new look at the problem of the mixture of the $3d$ and $4f$ magnetism at the very level of the exchange mechanisms.

APPENDIX: EXPRESSION OF THE GENERALIZED SUSCEPTIBILITY IN THE PRESENCE OF A QUADRUPOLAR EXCHANGE TERM

A calculation similar to that performed in Sec. III, with the addition of the quadrupolar Hamiltonian

(28) leads to the addition of the following terms to the formula (14): (1) easy magnetization direction along [110] axis

$$-(\tilde{g}_\lambda^{\alpha 1}-\tilde{g}_\lambda^{\alpha-1})\sum_{\lambda'}6G_{1\lambda'\lambda}(\vec{q})[\tilde{G}_{\lambda'\nu}^{-1\beta}(\vec{q},\omega)-\tilde{G}_{\lambda'\nu}^{1\beta}(\vec{q},\omega)]$$

$$-(\tilde{g}_\lambda^{\alpha 1}+\tilde{g}_\lambda^{\alpha-1})\sum_{\lambda'}\frac{G_{2\lambda'\lambda}(\vec{q})}{2}[\tilde{G}_{\lambda'\nu}^{-1\beta}(\vec{q},\omega)+G_{\lambda'\nu}^{1\beta}(\vec{q},\omega)]\ ;$$

(2) easy magnetization direction along [001] axis

$$-\tilde{g}_\lambda^{\alpha 1}\sum_{\lambda'}G_{2\lambda'\lambda}(\vec{q})\tilde{G}_{\lambda'\nu}^{-1\beta}(\vec{q},\omega)\qquad-\tilde{g}_\lambda^{\alpha-1}\sum_{\lambda'}G_{2\lambda'\lambda}(\vec{q})\tilde{G}_{\lambda'\nu}^{1\beta}(\vec{q},\omega)\ ,$$

with

$$\tilde{g}^{\alpha\gamma}=\sum_{mn}\frac{S_{mn}^{\alpha}O_{2nm}^{\gamma}(f_m-f_n)}{\omega-\omega_n+\omega_m}\ ,\quad\gamma=\pm1\ .$$

In the above formulas we have introduced the mixed generalized susceptibility

$\tilde{G}_{\lambda\nu}^{\gamma\beta}(\gamma=\pm1)$

which is written

$$\tilde{G}_{\lambda\nu}^{\gamma\beta}(\vec{q},\omega)=\tilde{g}_\lambda^{\gamma\beta}(\omega)\delta_{\lambda\nu}-\tilde{g}_\lambda^{\gamma+}(\omega)\left[\sum_{\lambda'}J_{\lambda'\lambda}(\vec{q})G_{\lambda'\nu}^{-\beta}(\vec{q},\omega)+\sum_{\mu}J_{\mu\lambda}(\vec{q})G_{\mu\nu}^{+\beta}(\vec{q},\omega)\right]$$

$$-\tilde{g}_{\lambda'}^{\gamma-}(\omega)\left[\sum_{\lambda'}J_{\lambda'\lambda}(\vec{q})G_{\lambda'\nu}^{+\beta}(\vec{q},\omega)+\sum_{\mu}J_{\mu\lambda}(\vec{q})G_{\mu\nu}^{-\beta}(\vec{q},\omega)\right]\ ,$$

with the addition of the supplementary terms depending on the cases (1) and (2) written above

$$\left.\begin{aligned}&-(\tilde{\tilde{g}}_\lambda^{\gamma 1}-\tilde{\tilde{g}}_\lambda^{\gamma-1})\sum_{\lambda'}6G_{1\lambda'\lambda}(\vec{q})[\tilde{G}_{\lambda'\nu}^{-1\beta}(\vec{q},\omega)-\tilde{G}_{\lambda'\nu}^{1\beta}(\vec{q},\omega)]\\&-(\tilde{\tilde{g}}_\lambda^{\gamma 1}+\tilde{\tilde{g}}_\lambda^{\gamma-1})\sum_{\lambda'}\frac{G_{2\lambda'\lambda}(\vec{q})}{2}[\tilde{G}_{\lambda'\nu}^{-1\beta}(\vec{q},\omega)+\tilde{G}_{\lambda'\nu}^{1\beta}(\vec{q},\omega)]\end{aligned}\right\}\qquad\text{(A1)}$$

$$-\tilde{\tilde{g}}_\lambda^{\gamma 1}\sum_{\lambda'}G_{2\lambda'\lambda}(\vec{q})\tilde{G}_{\lambda'\nu}^{-1\beta}(\vec{q},\omega)-\tilde{\tilde{g}}_\lambda^{\gamma-1}\sum_{\lambda'}G_{2\lambda'\lambda}(\vec{q})\tilde{G}_{\lambda'\nu}^{1\beta}(\vec{q},\omega)\qquad\text{(A2)}$$

with

$$\tilde{\tilde{g}}^{\gamma\gamma'}=\sum_{m,n}\frac{O_{2mn}^{\gamma}O_{2nm}^{\gamma'}(f_m-f_n)}{\omega-\omega_n+\omega_m}\ .$$

[1]R. M. Nicklow, N. C. Koon, C. M. Williams, and J. B. Milstein, Phys. Rev. Lett. 36, 532 (1976).

[2]J. J. Rhyne, N. C. Koon, J. B. Milstein, and H. A. Alperin, Physica (Utrecht) 86–88B, 149 (1977).

[3]N. C. Koon, B. N. Das, and J. J. Rhyne, J. Appl. Phys. 50, 1969 (1979).

[4]N. C. Koon and J. J. Rhyne, J. Magn. Magn. Mater. 15–18, 349 (1980).

[5]B. Barbara, D. Gignoux, D. Givord, F. Givord, and R. Lemaire, Int. J. Magn. 4, 77 (1973).

[6]R. Lemaire, Cobalt (Fr. Ed.) 33, 201 (1966).

[7]F. Givord and J. S. Shah, C. R. Acad. Sci. Ser. B 274, 923 (1972).

[8]G. Petrich and R. L. Mössbauer, Phys. Lett. A 26, 403 (1968).

[9]E. P. Wohlfarth and P. Rhodes, Philos. Mag. 7, 1817 (1962).

[10]M. Cyrot and M. Lavagna, J. Phys. (Paris) 40, 763 (1979).

[11]D. Gignoux, F. Givord, and R. Lemaire, Phys. Rev. B 12, 3878 (1975).

[12]G. Aubert, D. Gignoux, F. Givord, R. Lemaire, and B. Michelutti, Solid State Commun. 25, 85 (1978).
[13]A. Castets, D. Gignoux, and B. Hennion, J. Magn. Magn. Mater. 15–18, 375 (1980).
[14]W. J. L. Buyers, T. M. Holden, and A. Perreault, Phys. Rev. B 11, 266 (1975).
[15]W. Marshall and S. W. Lovesey, *Theory of Thermal Neutron Scattering* (Oxford University, London, 1971).
[16]K. R. Lea, M. J. M. Leask, and W. P. Wolf, J. Phys. Chem. Solids 23, 1381 (1962).
[17]M. Shimizu and H. Yamada, J. Phys. Soc. Jpn. 44, 1521 (1978).
[18]D. Gignoux, F. Givord, R. Perrier de la Batie, and F. Sayetat, J. Phys. F 9, 763 (1979).
[19]P. M. Levy, P. Morin, and D. Schmitt, Phys. Rev. Lett. 42, 1417 (1979).
[20]P. Morin and D. Schmitt, J. Phys. F 8, 951 (1978).
[21]J. J. Rhyne, N. C. Koon, and B. N. Das, J. Magn. Magn. Mater. 14, 273 (1979).
[22]N. C. Koon and J. J. Rhyne, Phys. Rev. B 23, 207 (1981).
[23]D. Gignoux and F. Givord, J. Phys. F 9, 1409 (1979).